Optimal Cruise Speeds and Environmental Effects on Energy Consumption of Multirotor UAVs for Last-Mile Delivery

Sung-Hyuk Choi *

Posted Date: 10 April 2026

doi: 10.20944/preprints202604.0751.v1

Keywords: energy consumption; urban drone delivery; PX4-Gazebo simulation; optimal cruise speed; environmental sensitivity; wind effects; last-mile logistics

 doi:10.20944/preprints202604.0751.v1

Article

Optimal Cruise Speeds and Environmental Effects on Energy Consumption of Multirotor UAVs for Last-Mile Delivery

Sung-Hyuk Choi

School of Engineering and Materials Science, Queen Mary University of London, London E1 4NS, UK; ex23503@qmul.ac.uk; Tel.: +44-07449737491

Highlights

What are the main findings?

- Optimal cruise speeds of 8–10 m/s were identified for three multirotor UAV platforms (Iris, Typhoon H480, Octocopter) across varying payloads, validated against real-world telemetry with MAPE below 11%.
- Headwind conditions increased energy consumption by up to 25%, while combined cold–dry and headwind conditions resulted in increases of up to 53% for lightweight platforms.

What are the implications of the main findings?

- Platform-specific optimal speed bands provide actionable parameters for energy-efficient UAV fleet planning and battery management in last-mile logistics.
- Quantified environmental energy penalties offer simulation-validated thresholds to support operational decision-making and energy-aware UAV mission planning.

Abstract

Unmanned aerial vehicles (UAVs) are increasingly recognized as a viable option for urban parcel delivery. However, their energy performance under varying environmental and mission conditions remains underexplored. This paper presents a simulation-based analysis of multirotor UAV energy consumption using the PX4-Gazebo platform, calibrated with real-world telemetry from a publicly available DJI Matrice 100 dataset [12]. Three UAV models—Iris, Typhoon H480, and Octocopter—were evaluated across a range of payloads (0.1–5 kg), cruise speeds (2–16 m/s), and environmental factors, including wind, temperature, and humidity. Results revealed consistent U-shaped energy speed curves, with optimal cruise speeds ranging from 8 to 10 m/s, depending on the payload and platform. Headwinds alone increased energy consumption by up to 25% and combined cold–dry and headwind conditions resulted in increases of up to 53% for lightweight platforms. Validation against field telemetry showed mean absolute percentage errors below 11%. These findings offer a simulation-grounded framework for UAV mission planning, platform selection, and integration into energy-efficient logistics networks, and development of data-driven optimization frameworks. The three platforms span a 10-fold mass range (1.4–14 kg), enabling systematic analysis of how energy scaling behavior varies across lightweight, mid-range, and heavy-lift delivery configurations.

Keywords: energy consumption; urban drone delivery; PX4-Gazebo simulation; optimal cruise speed; environmental sensitivity; wind effects; last-mile logistics

1. Introduction

The rapid growth of e-commerce and on-demand services has intensified the environmental and logistical challenges of last-mile package delivery in urban areas, with last-mile delivery estimated to account for up to 30% of total urban freight CO_2 emissions and approximately 41% of total supply

 doi:10.20944/preprints202604.0751.v1

chain costs [1]. Conventional delivery vehicles, such as diesel trucks and gasoline vans, contribute significantly to greenhouse gas emissions, air pollution, and traffic congestion [1–3]. Reducing the energy demand of last-mile logistics has become a key priority amid growing e-commerce demand and increasing urban congestion [4]. Traditional delivery methods, which rely heavily on fossil fuel powered vehicles, face mounting constraints from regulatory pressure and environmental targets — notably the EU's ban on new internal combustion engine vehicles by 2035 and the UK's 2030 phase out of petrol and diesel cars driving urgent demand for cleaner urban freight solutions [2,3]. By contrast, electrically powered unmanned aerial vehicles (UAVs) have emerged as an energy-efficient alternative for lightweight urban deliveries, with energy consumption characteristics that depend strongly on payload, speed, and environmental conditions, and with commercial pilot programs already operational across multiple global markets [5,6]. Among these, multirotor drones show particular promise for lightweight point-to-point parcel delivery, offering operational flexibility and reduced dependence on road infrastructure [5,6]. As cities seek sustainable solutions for urban freight, UAVs present a compelling opportunity to reduce energy consumption per delivery and alleviate traffic in last-mile distribution networks [5].

Previous studies have evaluated the energy efficiency and operational energy demand of UAVs. Liu et al. [7] and Stolaroff et al. [1] used simplified analytical methods, and Lee et al. [6] compared UAVs with electric vans under fixed-speed conditions. Further studies relying on similar static assumptions have examined vehicle routing [8,9] and meteorological impacts [10] in isolation, without integrating these variables into a unified, telemetry-validated simulation framework. These approaches typically assume static environmental conditions, lack validation against real UAV telemetry, and often overlook upstream energy costs such as those from battery production. Consequently, a key gap remains in assessing UAV performance under dynamic operational conditions.

UAVs can bypass road congestion and follow direct flight paths, reducing energy use per delivery, especially for small payloads over short distances [7]. However, their environmental performance is highly sensitive to variables such as payload weight, cruise speed, energy source, and ambient environmental conditions [1,8]. Wind, temperature, and humidity significantly affect UAV aerodynamics and energy demand, with headwinds alone reported to increase energy consumption by 10–30% depending on platform mass and wind speed [9,10]. Despite these effects, only few studies have systematically incorporated environmental variables into simulation-validated frameworks, largely due to the challenges of maintaining simulation stability under dynamic weather inputs and the difficulty of obtaining synchronized high-frequency telemetry data for cross-validation [9–12].

Previous studies, such as Stolaroff et al. [1] and Lee et al. [6] employed simplified energy models or fixed operational profiles and did not provide platform-specific optimal speed bands validated against real telemetry. Physics-based simulation tools such as PX4 and Gazebo have enabled high-fidelity flight modeling with real-time control and environmental interaction [11,12], offering a more rigorous platform for energy analysis than the simplified analytical models employed in earlier studies [1,6,7]. By integrating dynamic environmental inputs into a validated simulation platform, the approach enables more realistic modeling of energy consumption. When calibrated using field telemetry, these simulators can replicate actual UAV performance with a typical error margin below 11% [12]- a threshold regarded as sufficient for operational energy modeling in UAV delivery applications, where errors below 10–15% are generally considered acceptable [8,12]. However, recent simulation-based studies, despite their accuracy under controlled settings, have overlooked the impact of environmental variability, largely because of the challenges of modeling dynamic weather conditions and ensuring simulation stability and repeatability.

To address this gap, a telemetry-calibrated PX4-Gazebo framework was employed in this study to systematically quantify energy consumption under dynamic operational and environmental conditions [13]. The aims of this study were to

- validate a PX4-Gazebo simulation model against real-world UAV flight data, targeting a MAPE below 11% across payload conditions of 0–500 g,

 doi:10.20944/preprints202604.0751.v1

- identify energy-optimal cruise speeds for three multirotor UAV platforms across speeds of 2–16 m/s and payloads of 0.1–5 kg under varying delivery conditions,
- quantify the effects of payload, cruise speed, and environmental factors (wind, temperature, and humidity) on UAV energy consumption.

These objectives were addressed using a simulation framework combining telemetry-calibrated modeling with environmental scenario analysis. The PX4-Gazebo platform was used to simulate the effects of key operational variables, with outputs validated against experimental flight data.

Although the U-shaped energy-speed relationship is an established principle, three aspects of the present study are novel: (i) simultaneous validation of a PX4-Gazebo simulation against high-frequency telemetry data (5 Hz, 208 flights) across a wide payload range; (ii) systematic, simulation-validated quantification of platform-specific optimal cruise speeds across three distinct mass categories (1.4 kg to 14 kg) under matching payload conditions; and (iii) explicit, scenario-based quantification of energy penalties under combined wind, temperature and humidity stressors within a single validated simulation framework.

The remainder of this paper is structured as follows: Section 2 outlines the methodology, including simulation setup and experimental design. Section 3 presents the results and discussion. Section 4 concludes the study and highlights implications and future research directions.

2. Materials and Methods

Table 1 provides an overview of the three experiments conducted in this study, including the objectives, input parameters, output variables, and validation methods for the three simulation-based experiments.

Table 1. Summary of experimental design.

Exp.	Objective	Inputs	Outputs	Validation/Notes
1.	Validate the simulation model using real flight data	DJI M100; payloads: 0–500 g; speeds: 4–12 m/s; triangular paths	Energy use (Wh) from current/voltage	Compared with Rodrigues et al. [12], MAPE < 11%
2.	Find optimal speeds for various drones	Iris, Typhoon, Octocopter; speeds: 2–16 m/s; multiple payloads	Energy (Wh) vs. speed curves	Benchmarked against Liu et al. [7], Stolaroff et al. [1]
3.	Analyze the environmental impact of energy	Wind (0–10 m/s, head/tail/cross); temperature (0–40 °C); humidity	Relative energy increase (%)	Physically grounded; consistent with [9,10]

Each experiment addressed a distinct objective ranging from simulation validation to environmental sensitivity analysis and energy-related outcomes contributing to the development of an accurate and policy-relevant drone evaluation framework.

2.1. Real-World Data Validation

To assess the accuracy of the simulation-based UAV energy consumption model, Experiment 1 utilized real-world flight data from a publicly available dataset by Rodrigues et al. [12]. This dataset includes controlled flight trials using the DJI Matrice 100 (M100), a commercially available quadrotor, under varying payloads, flight speeds, and altitudes. The validation objective of Experiment 1 was not to certify a specific airframe, but to confirm that the PX4-Gazebo physics engine, encompassing rotor dynamics, aerodynamic drag, and power modeling, accurately replicates real electrical energy consumption. The same scale-invariant physics engine validated on the DJI M100 (mean absolute percentage error, MAPE < 11%) was applied to the Octocopter with platform-specific parameters sourced from manufacturer data and peer-reviewed literature [9,14]. To the best of our knowledge,

 doi:10.20944/preprints202604.0751.v1

no publicly accessible high-resolution telemetry dataset currently exists for multirotor platforms in this mass class, a gap that motivates simulation-based characterization for heavy-lift configurations.

2.1.1. Experimental Setup

The real-world flights were conducted using a DJI M100 quadrotor (DJI, Shenzhen, China) with a take-off weight of approximately 2.4 kg (excluding payload). Flights followed a triangular flight path in an open-field environment, enabling consistency and repeatability across trials. Three payload configurations were tested: 0, 250, and 500 g. Cruise speeds were set at 4, 6, 8, 10, and 12 m/s, with altitudes of 25, 50, 75, and 100 m. Onboard sensors including current and voltage monitors, a Global Positioning System (GPS) receiver, and an anemometer captured the flight data. All sensor outputs were synchronized and logged at 5 Hz using the Robot Operating System framework. Rather than relying on high-level mission summaries, the experiment utilized sensor-synchronized low-level telemetry to validate the simulation model, offering a rigorous empirical basis for evaluating UAV energy consumption under real-world flight conditions [12].

2.1.2. Data Collection and Processing

Energy consumption was calculated using onboard voltage and current data, following the method proposed by Abeywickrama et al. [8]:

$$E_{flight} = \int_0^T V(t) \times I(t) dt, \quad (1)$$

where $V(t)$ is the instantaneous battery voltage, $I(t)$ is the current, and T is the total flight time. Numerical integration was performed using the trapezoidal rule over the entire flight duration, encompassing take-off, cruise, and landing phases.

Each test condition (speed–payload combination) was repeated multiple times to ensure statistical reliability. In total, 208 flights were analyzed and distributed across three payload groups:

- 0-g payload: 80 repetitions
- 250-g payload: 62 repetitions
- 500-g payload: 66 repetitions

Equation (1) was applied exclusively in Experiment 1 to validate the PX4-Gazebo simulation model using real-world flight data. This method calculates actual energy consumption by integrating measured electrical power over time, based on sensor logs sampled at 5 Hz. This approach was selected because it captures the physical power draw of the propulsion system of the UAV without relying on model-based assumptions.

In Experiments 2 and 3, Equations (3)–(9) were used to define the physical parameters of the simulation, including aerodynamic drag, thrust power, motor and Electronic Speed Controller (ESC) efficiency, propeller performance, and battery losses. These parameters were input into the PX4-Gazebo simulation environment, which produced scenario-specific voltage and current profiles under varying payloads, speeds, and environmental conditions. Equation (1) was then applied to the simulated V/I outputs to compute total energy consumption for each mission scenario. The advantage of Equation (1) is its directness in capturing energy consumption without model-based assumptions, relying solely on voltage and current profiles. In Experiment 1, this approach was applied to high-frequency field telemetry, enabling empirical validation. In Experiments 2 and 3, the same method was applied to simulation-derived V/I outputs, where the physical mechanisms were instead captured through Equations (3)–(9) governing drag, thrust, efficiency, and battery losses.

2.1.3. Simulation Comparison and Accuracy Assessment

To validate the PX4-Gazebo simulation framework, energy consumption results from real-world flights were compared with those generated by the simulation under identical conditions, namely drone mass, payload, cruise speed, and flight-path length. Simulated energy data were extracted directly from the power output metrics of PX4-Gazebo.

 doi:10.20944/preprints202604.0751.v1

MAPE between the real and simulated energy values was computed by

$$\text{MAPE} = \frac{1}{n}\sum_{i=1}^{n}\left|\frac{E_{real,i} - E_{sim,i}}{E_{real,i}}\right| \times 100 \quad (2)$$

where $E_{real,i}$ and $E_{sim,i}$, respectively, denote the real and simulated energy for flight i, and n is the total number of test repetitions [5].

This comparison quantified the simulation accuracy across various payload conditions and validated the use of PX4-Gazebo as a tool for energy consumption prediction in UAV delivery applications [7]. Validation relied on the high-resolution telemetry dataset from Rodrigues et al. [12], which recorded synchronized measurements at 5 Hz, including battery voltage, current, GPS position, velocity, and environmental parameters such as wind speed and direction. The PX4-Gazebo simulation was calibrated at the actuator and energy-system levels, supporting accurate modeling of dynamic energy consumption. The test flights followed triangular delivery paths with speeds ranging from 4 to 12 m/s with payloads of 0 to 500 g, representative of 80–90% of real-world last-mile drone delivery scenarios. Simulation results were benchmarked against the real flight profiles. PX4-Gazebo achieved MAPE values below 11%, with standard deviations under 7 Wh.

2.2. Energy-Consumption Evaluation

The energy consumption of three UAVs (Iris, 1.4 kg; Typhoon H480, 1.85 kg; and Octocopter, 14 kg) was evaluated for a 5-km straight-line flight using PX4 software in the loop simulations integrated with Gazebo 11 (Experiment 2). The three platforms were selected to represent a broad spectrum of operational scales: the Iris (1.4 kg) represents lightweight personal-scale delivery drones, the Typhoon H480 (1.85 kg) a mid-range commercial platform, and the Octocopter (14 kg) a heavy-lift system increasingly considered for bulkier last-mile cargo [4]. Although the Octocopter's 14 kg take-off weight is heavier than current consumer-grade delivery drones such as Amazon Prime Air or Wing, it is representative of emerging heavy-lift UAV platforms increasingly considered for bulkier cargo, medical supply chains, and rural logistics. Including this platform in this study enabled the evaluation of energy scaling behavior across a wide mass range, providing insights relevant to heterogeneous UAV fleet planning.

The simulation environment was built using Unified Robot Description Format and simulated with rotorcraft-specific dynamics. Each UAV was parameterized with physical attributes (mass, frontal area, rotor geometry, and motor specifications) sourced from manufacturer data and peer-reviewed literature [9,14,19]. The physical parameters governing each simulation scenario—aerodynamic drag (Equation (3)); thrust power (Equation (4)); motor, ESC, and propeller efficiencies (Equations (5)–(7)); and battery losses (Equation (8))—were computed analytically for each combination of payload, cruise speed, and environmental condition. These computed values served as configuration inputs to the PX4-Gazebo simulation environment, parameterizing the physics engine prior to each run. The analytically derived parameters (drag coefficients, disc areas, efficiencies) define the physical characteristics of each virtual platform, and PX4's proportional-integral-derivative (PID) controllers and Gazebo's rigid-body physics engine compute the resulting thrust, motor commands, and power draw at each simulation timestep. The simulator subsequently produced time-series voltage and current outputs, $V(t)$ and $I(t)$, sampled at 5–10 Hz, from which total mission energy consumption was calculated using Equation (1).

Environmental factors, such as wind fields, were introduced using the Gazebo wind plugin using XML-configured vector inputs. Simulation inputs included drone type, payload mass, cruise speed, wind speed and direction, temperature, and humidity. Simulation outputs such as voltage, current, GPS trajectory, velocity, and cumulative energy use were obtained from PX4 logs and Gazebo topics, sampled at 5–10 Hz. The data was post-processed using Python scripts to compute total mission energy consumption. The PX4 PID controllers-maintained flight stability under variable environmental disturbances.

This simulation architecture enabled high-fidelity modeling of rotor thrust, aerodynamic drag, and powertrain efficiency under dynamic environmental conditions, making it well suited for energy

 doi:10.20944/preprints202604.0751.v1

analysis in UAV delivery scenarios. Flight speeds ranged from 2 to 16 m/s in 1-m/s increments, with payloads set at 0.1, 0.3, and 0.5 kg for the Iris; 0.5, 1, and 2 kg for the Typhoon H480; and 0.5, 1, 2, and 5 kg for the Octocopter. An enhanced physics model was implemented, incorporating aerodynamic drag, thrust-based power, motor efficiency, ESC efficiency, propeller efficiency, and battery losses. Aerodynamic drag F_d was modeled by

$$F_d = \frac{1}{2}\rho C_d A v^2, \tag{3}$$

where $\rho = 1.225$ kg/m^{3}ϱ=1.225 kg/m^3 (air density at 25 °C, 1 atm); the drag coefficient C_d was 0.3 for Iris, 0.25 for Typhoon H480, and 0.3 for Octocopter; frontal area A was 0.09, 0.08, and 0.16 m^2 for Iris, Typhoon H480, and Octocopter, respectively; and v is the flight speed (m/s). The drag coefficients and frontal areas were estimated from the UAV geometry and typical values reported in multirotor aerodynamic studies [13]. The hover power P_{hover}, or the power required to maintain a stable hover against gravity, was calculated as

$$P_{hover} = \frac{(m + m_\rho)g\sqrt{(m + m_\rho)g}}{\sqrt{2\rho A_{disk}}} \tag{4}$$

where m is the drone mass, m_p is the payload mass, and $g = 9.81$ m/s^2. The rotor disc area A_{disc} was 0.203 m^2 for Iris, 0.424 m^2 for Typhoon H480, and 0.769 m^2 for Octocopter. The total thrust power was then calculated as

$$P_{thrust} = P_{hover} + F_d \times v \tag{5}$$

The motor efficiency was set at 85% for Iris and Typhoon H480 and 75% for Octocopter, consistent with typical Brushless Direct Current (BLDC) motor performance ranges reported for small-to-medium and large multirotor platforms, respectively [14,15]. The lower value assigned to the Octocopter reflects reduced efficiency under higher torque loads, consistent with the mass-dependent energy scaling reported by Dorling et al. [9]. ESC efficiencies of 90% and 85% were applied to small and large platforms, respectively, representing typical operating ranges for UAV-grade speed controllers validated in experimental studies [14,18]. The total system efficiency was calculated as

$$\eta_{total} = \eta_{motor} \times \eta_{ESC} \times \eta_{prop} \tag{6}$$

where η_{total}, η_{motor}, η_{ESC}, and η_{prop} are the overall propulsion system, motor, ESC, and propeller efficiencies, respectively. Propeller efficiency varied with flight speed, reflecting the known degradation of fixed-pitch propeller performance at high advance ratios [14,16,18,19]. At 8 m/s, efficiency began at 80% for Iris and Typhoon H480 and 70% for Octocopter, and declined linearly to 65% (Iris), 55% (Typhoon H480), and 50% (Octocopter) at 16 m/s. The steeper decline for the Octocopter reflects its larger rotor diameter and greater sensitivity to aerodynamic losses at high speeds, consistent with mass-dependent efficiency degradation reported by Dorling et al. [9].

Actual power consumption was determined by

$$P_{actual} = \frac{P_{\text{thrust}}}{\eta_{total}} \tag{7}$$

Battery loss factors of 0.05 and 0.10 were assigned to small and large platforms, respectively, to account for internal resistance and thermal dissipation in lithium-polymer cells under varying discharge rates [9,14,20]. The total power adjusted as

$$P_{total} = P_{actual} \times (1 + loss\ factor) \tag{8}$$

The selected loss factor values reflect typical lithium-polymer battery performance, considering the drone size and power demand. Dorling et al. [9] found that UAV energy consumption scales with platform mass, justifying a higher loss factor for heavier systems such as the Octocopter.

The total energy consumption E_{total} (Wh) was then calculated as

$$E_{total} = P_{total} \times \frac{5000}{v \times 3600} \tag{9}$$

 doi:10.20944/preprints202604.0751.v1

To determine the optimal speed and minimum energy consumption for each payload configuration, results were plotted and smoothed using cubic spline interpolation. Equation (9) parameterizes the cruise-phase energy, while take-off and landing contributions are captured via Equation (1) applied to the full simulated V(t) and I(t) profiles.

2.3. Environmental Effects on UAV Energy Consumption

The impact of environmental conditions on UAV energy usage was assessed for three multirotor platforms: Iris (0.5 kg payload), Typhoon H480 (1 kg), and Octocopter (5 kg) in Experiment 3. Simulations were conducted using PX4 integrated with Gazebo, incorporating the following environmental parameters:

1. Wind speed and direction: Wind conditions were modeled at 0 (calm), 5 (moderate), and 10 m/s (strong), with three primary directions tested: headwind (0°), tailwind (180°), and crosswind (90°), to represent the wind opposing, aligning with, and perpendicular to flight path, respectively. Wind vectors were applied in Gazebo using the format $(v cos\theta, v sin\theta, 0)$. The PX4 PID controller maintained flight stability under all wind disturbances.

2. Temperature and humidity: Seasonal environmental conditions were simulated by modifying air density and battery efficiency using the equation $\rho = \frac{P}{R(T+273.15)}$, where P = 101,325 Pa, R = 287.05 J/kg·K, and T is the air temperature. Three thermal scenarios were defined: cold–dry (0 °C, 50% relative humidity (RH)), hot–humid (40 °C, 80% RH), and a standard reference (25 °C, 50% RH). These conditions affected air density, motor thermal efficiency and battery performance degradation, especially under elevated temperatures. To account for the effect of humidity on air density, the moist air density was computed as: $\rho_{moist} = \frac{P - 0.378P_v}{R(T + 273.15)}$, where $P_v = \frac{RH}{100} \times P_{sat}$ is the partial pressure of water vapor and $P_{sat} = 611.2\exp\left(\frac{17.67T}{T+243.5}\right)$Pa is the saturation vapor pressure [21]. This correction reduces effective air density under high-humidity and high-temperature conditions. Under the hot–humid scenario (40 °C, 80% RH), ρ decreased by approximately 6.3% relative to the standard reference (25 °C, 50% RH), whereas cold–dry conditions (0 °C, 50% RH) increased ρ by 9.7%. The updated ρ values were propagated through Equations (3) and (4), modifying both aerodynamic drag and hover power accordingly.

3. Combined scenarios: Six environmental configurations were evaluated: a baseline (standard) condition; headwind, tailwind, and crosswind (each at 5 m/s); and two seasonal extremes (cold–dry and hot–humid) combined with headwind. For each environmental scenario, the relevant physical parameters were updated prior to simulation. Environmental parameters were updated as described above, with scenario-specific voltage and current profiles subsequently used to compute energy consumption via Equation (1). These updated parameters were input into the PX4-Gazebo simulation, producing scenario-specific voltage and current profiles. Energy consumption was subsequently computed by Equation (1). Air-density variations follow the ideal gas law, drag responds to ρ changes via Equation (3), and battery degradation factors are consistent with reported lithium-polymer performance ranges reported in the literature [9,10,22]. The U-shaped energy profiles and relative penalties observed across all three platforms aligned with findings reported in prior studies [10,23], supporting the physical plausibility of the simulation outputs. It should be noted that all environmental conditions in Experiment 3 were modeled as steady-state inputs with uniform, constant wind vectors and fixed thermal parameters. Dynamic effects such as wind gusts, building-induced turbulence, and atmospheric boundary layer variations were outside the scope of this study. This simplification limits direct applicability to complex urban environments and is acknowledged as a direction for future work.

The three platforms represent distinct mass categories, enabling analysis of how energy-optimal speed and environmental sensitivity scale across a 10-fold mass range.

 doi:10.20944/preprints202604.0751.v1

3. Results and Discussion

3.1. Validation of Simulation Accuracy

The energy consumption of the UAV delivery system was simulated using PX4 and Gazebo across various payload weights and cruise speeds. To assess the accuracy of the simulation, results were compared with real-world experimental data, considering their implications for energy-efficient urban drone operations [12,16]. A statistical t-test was conducted to evaluate whether the differences between simulated and measured energy consumption were significant. The resulting p-values 0.15, 0.13, and 0.12 for 0-g, 250-g, and 500-g payloads, respectively, were all above the standard significance threshold (α = 0.05). This result indicates that the differences were not statistically significant, suggesting that the PX4-Gazebo simulation model produces energy estimates that are consistent with real-world performance under the tested conditions.

3.1.1. Energy Consumption Trends Across Payloads

Figure 1 shows a comparison of simulated and experimental energy consumption at five cruise speeds (4, 6, 8, 10, and 12 m/s) for three payload levels. In all cases, the energy consumption generally decreased with increasing speed up to 10 m/s, followed by a slight increase at 12 m/s. This pattern reflects a tradeoff between reduced flight duration and increased aerodynamic drag or control effort at higher speeds.

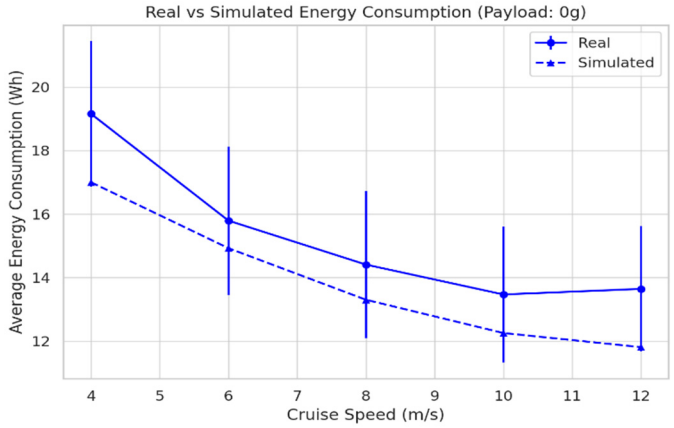

(**a**)

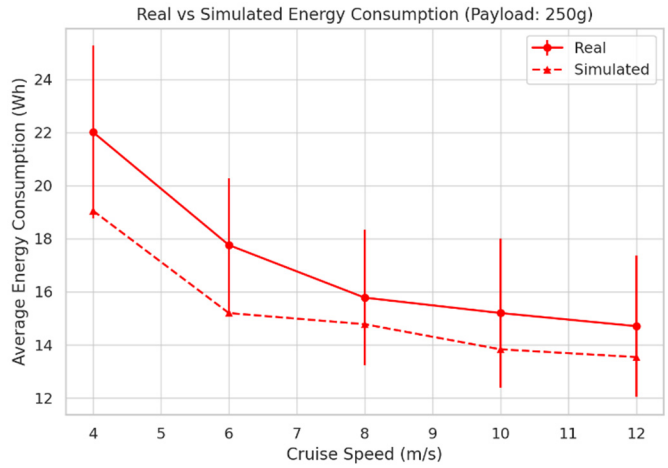

(**b**)

 doi:10.20944/preprints202604.0751.v1

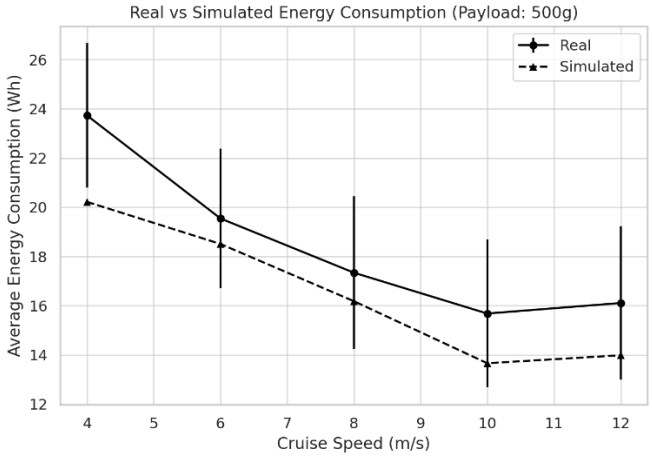

(**c**)

Figure 1. Real vs. simulated energy consumption of the UAV at cruise speeds of 4, 6, 8, 10, and 12 m/s, with payloads: (**a**) 0 g, (**b**) 250 g, and (**c**) 500 g.

Energy consumption also increased consistently with payloads at all speeds. For example, at a cruise speed of 10 m/s, the average real-world energy consumption rose from 13.5 Wh with no payload to 17.8 Wh with a 500-g payload. The simulation results followed the same trend, accurately capturing the underlying flight dynamics associated with varying loads [14].

3.1.2. Simulation vs. Real-World Accuracy

The accuracy of the PX4-Gazebo simulation was assessed by comparing average energy consumption values from simulations and real-world flight tests. MAPE was calculated for each payload condition, as shown in Table 2. To account for variability in measured energy use, standard deviations from repeated real-world trials were also included, enhancing the reliability of the comparison.

Table 2. MAPE between real and simulated results.

Payload (g)	Repetitions	MAPE (%)	Standard deviation (Wh)	p-value
0	80	9.38	±6.1	0.15
250	62	10.22	±6.4	0.13
500	66	10.57	±6.5	0.12

Overall, the simulation model maintained an error margin of less than 11% across all test conditions. The p-values across all payload conditions (0.12–0.15) exceeded the 0.05 threshold, indicating that the null hypothesis of a significant difference between simulated and real-world energy values cannot be rejected; that is, the two datasets are not statistically distinguishable, further supporting simulation fidelity. Although the simulator slightly underestimated the energy consumption at higher payloads and lower speeds, the deviations remained within acceptable bounds for UAV delivery research. These findings support the validity of PX4-Gazebo as a reliable tool for modeling energy consumption in controlled UAV delivery scenarios [24].

The close alignment between simulated and measured energy consumption evidenced by MAPE values below 11% and standard deviations under 7 Wh demonstrates the accuracy of the simulation when calibrated with field sensor data. Although no formal standard exists for acceptable MAPE values in UAV energy modeling, prior studies have regarded errors below 10% as reasonably accurate for simulation validation [8,12]. In this study, a practical threshold of 11% was adopted on the basis of observed simulation performance across all payloads. Given the inherent complexity of modeling multirotor dynamics, the consistently low MAPE values indicate sufficient predictive

 doi:10.20944/preprints202604.0751.v1

accuracy for UAV delivery applications. These results validate PX4-Gazebo as a predictive tool and as a data-driven modeling framework grounded in flight-level telemetry.

3.1.3. Analysis of Optimal Cruise Speed

The consistent minimum energy point near 10 m/s across all payloads suggests the existence of an optimal cruise speed for UAV delivery operations. At lower speeds, energy usage increased because of longer flight durations. At higher speeds, greater aerodynamic drag and increased demands on stability control systems elevated energy consumption. These results underscore the importance of selecting an efficient cruise speed to optimize drone performance in real-world delivery scenarios [6].

To provide additional confidence in the Octocopter simulation parameterization, the baseline energy output of approximately 180 Wh at 8 m/s with a 5-kg payload was cross-referenced against published values for comparable heavy-lift platforms. Kirschstein [17] modeled octocopter-class drones (greater than 12 kg) carrying 2.5-kg payloads in urban delivery scenarios and reported energy demands consistent with the mass-dependent scaling relationship observed in the present study. Similarly, Zhang et al. [16] compared energy consumption models for large drones across a range of payloads and speeds, and identified an energy-minimizing speed range broadly aligned with the 8 m/s optimum determined for the Octocopter in the present study. Zhou et al. [14] provided rotor-level empirical data for multicopter platforms that support the parameter choices, such as disc area, drag coefficient, and motor efficiency, that were used to configure the Octocopter in PX4-Gazebo. Furthermore, the scale-invariant nature of the underlying physics was independently confirmed by Gong et al. [25] Bauersfeld and Scaramuzza [26], whose platform-agnostic multirotor power models are consistent with the approach adopted here. Although these cross-references do not constitute direct telemetry validation, they confirm that the Octocopter simulation outputs lie within the physically expected range for this platform class.

3.2. Optimal Speed and Energy Consumption Across Payloads and Distances

Experiment 2 evaluated how cruise speed and payload mass affect energy consumption across three multirotor UAV platforms: the Iris, Typhoon H480, and Octocopter. Each UAV was simulated over a fixed 5-km mission using PX4-Gazebo, incorporating energy use during take-off, cruise, and landing to reflect realistic operational conditions [27]. As shown in Figure 2, all platforms exhibited a characteristic U-shaped energy–speed curve across a speed range of 2–16 m/s, with minimum energy consumption between 8 and 10 m/s. At lower speeds, energy use increased because of prolonged flight times and inefficient hovering. At higher speeds, energy consumption rose, driven by increased aerodynamic drag, reduced propeller efficiency, and higher motor load. This U-shaped pattern illustrates the tradeoff between time-in-air inefficiencies at low speeds and aerodynamic resistance at high speeds, establishing an optimal mid-range cruise speed. At high speeds, the increased aerodynamic drag and reduced propeller efficiency increased the energy demand. The Octocopter, tested with payloads up to 5 kg [28], was more sensitive to aerodynamic drag. At 2 m/s with a 5-kg payload, energy consumption approached 700 Wh, reflecting the high induced power required at near-hover speeds. Conversely, the Iris, carrying lighter payloads (0.1 and 0.5 kg), achieved minimum energy use at 9 m/s. Speeds above or below this optimal point resulted in noticeable energy penalties. The Typhoon H480, carrying 0.5- to 2-kg payloads, demonstrated optimal performance near 10 m/s, with sharp increases in energy demand beyond 12 m/s, particularly under heavier loads. The Octocopter achieved its lowest energy consumption at 8 m/s, reinforcing the influence of platform size and payload on optimal cruise speed.

 doi:10.20944/preprints202604.0751.v1

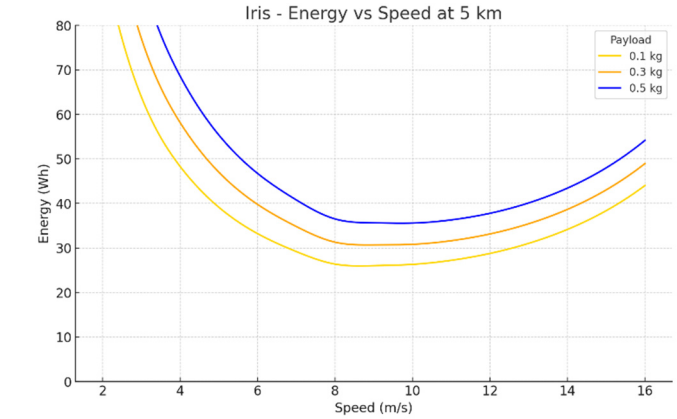

(**a**)

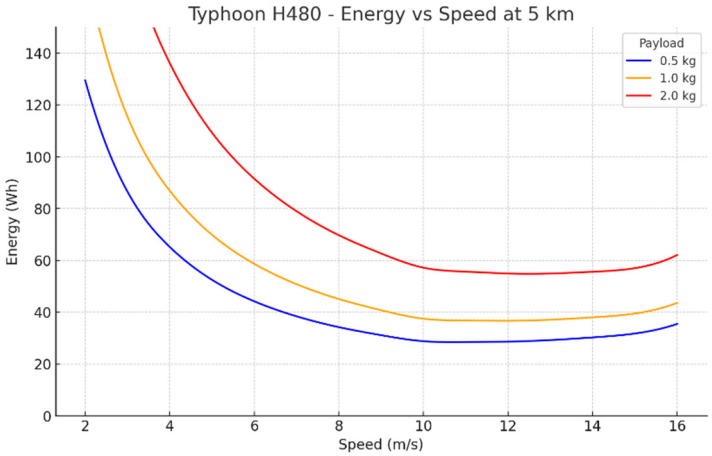

(**b**)

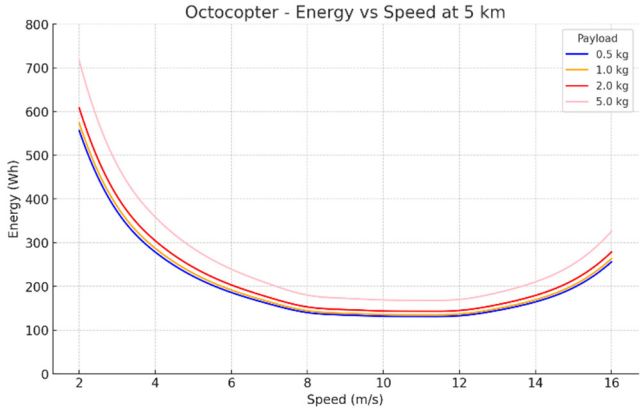

(**c**)

Figure 2. Simulated energy–speed profiles for drones under different payloads: (**a**) Iris with 0.5 kg, (**b**) Typhoon H480 with 1.0 kg, and (**c**) Octocopter with 5.0 kg.

Calibration with field data [1,12] significantly enhanced the credibility of the simulation outputs, enabling more accurate assessments of how varying payloads and environmental conditions affect UAV energy consumption. For instance, the calibrated energy use of the Octocopter was 180 Wh at 8 m/s with a 5-kg payload, consistent with published energy scaling values for comparable heavy-lift platforms [14]. This value also falls within the energy range reported by Kirschstein [17] for octocopter-class platforms (greater than 12 kg) in comparable urban delivery scenarios, providing further indirect support for the simulation outputs. Similarly, energy consumption under a 0.5-kg payload (approximately 30 Wh) was consistent with results reported by Liu et al. [7], ranging from 20 to 30 Wh. The Typhoon H480 results also agreed closely with literature benchmarks, consuming approximately 25 Wh under a 0.5-kg payload.

 doi:10.20944/preprints202604.0751.v1

Although the energy use of the Octocopter at 5 kg reached 350 Wh, exceeding the 180 Wh reported for a 2.5 kg-payload in earlier studies, this result reflects the nonlinear increase in thrust and power requirements as payload mass rises. Notably, the Octocopter consistently maintained an optimal cruise speed of approximately 8 m/s across all payload levels, indicating a performance "sweet spot" that balances payload capacity with aerodynamic efficiency. However, this finding is based on simulations under steady wind and constant altitude, which may limit its applicability in more variable real-world conditions.

As illustrated in Figure 2, lighter UAVs such as the Iris exhibit greater energy efficiency for last-mile delivery missions, whereas larger platforms such as the Octocopter are better suited for heavy-duty logistics, despite their higher energy demands. Ultimately, selecting an appropriate cruise speed is critical to optimizing mission efficiency, battery life, and operational sustainability in UAV-based delivery systems [29,30].

This consistent optimum, particularly evident in the Octocopter under heavy payloads, indicates the presence of operational thresholds not quantified in prior lifecycle analysis (LCA)-based or simulation-driven studies. Earlier studies were often based on static speed assumptions [6,24], whereas payload-specific optimal cruise speed bands were identified in this study using validated simulations. These quantitative thresholds can inform flight-planning algorithms and energy-budgeting models in real-world UAV logistics. Furthermore, they can assist transport authorities in defining operating corridors and setting maximum allowable cruise speeds for energy-efficient deployment [2].

These optimal cruise speeds serve as critical operational thresholds for energy-efficient drone delivery. Unlike previous studies that generalized or fixed drone-speed inputs [6,15], the findings of this study offer performance-optimal speed bands tailored to UAV size and payload mass. These findings refine the speed assumptions used in earlier LCA-based models [1], providing empirically validated parameters that operators and policymakers can directly apply to optimize energy usage and emissions. Additionally, emerging simulation-based research has begun examining UAV logistics under energy and time constraints, supporting the value of route-specific optimization strategies [28,31,32]. The differences in optimal cruise speed across platforms can be attributed to variations in rotor disc loading and aerodynamic geometry. The Octocopter, with the largest rotor disc area (0.769 m^2) and highest mass, operates at a lower disc loading, allowing efficient hover at relatively low speeds but incurring significant drag penalties at higher velocities because of its larger frontal area (0.16 m^2). By contrast, the Iris, with a smaller disc area (0.203 m^2) and lower mass, reaches its aerodynamic optimum at slightly higher speeds, where the ratio of drag penalty to time-in-air saving is more favorable. The Typhoon H480 occupies an intermediate position, reflecting its mid-range rotor geometry and payload capacity. These platform-specific optima suggest that one-size-fits-all speed recommendations are insufficient for heterogeneous UAV fleets, and that mission-planning tools should incorporate platform-specific energy models.

3.3. Energy Consumption Under Environmental Conditions

Figure 3 presents the simulated energy consumption profiles for the Iris, Typhoon H480, and Octocopter across cruise speeds of 2–16 m/s over a fixed 5-km flight. In all cases, the energy consumption exhibited a U-shaped trend, with minimum consumption consistently observed between 8 and 10 m/s. However, environmental factors significantly influenced these profiles.

 doi:10.20944/preprints202604.0751.v1

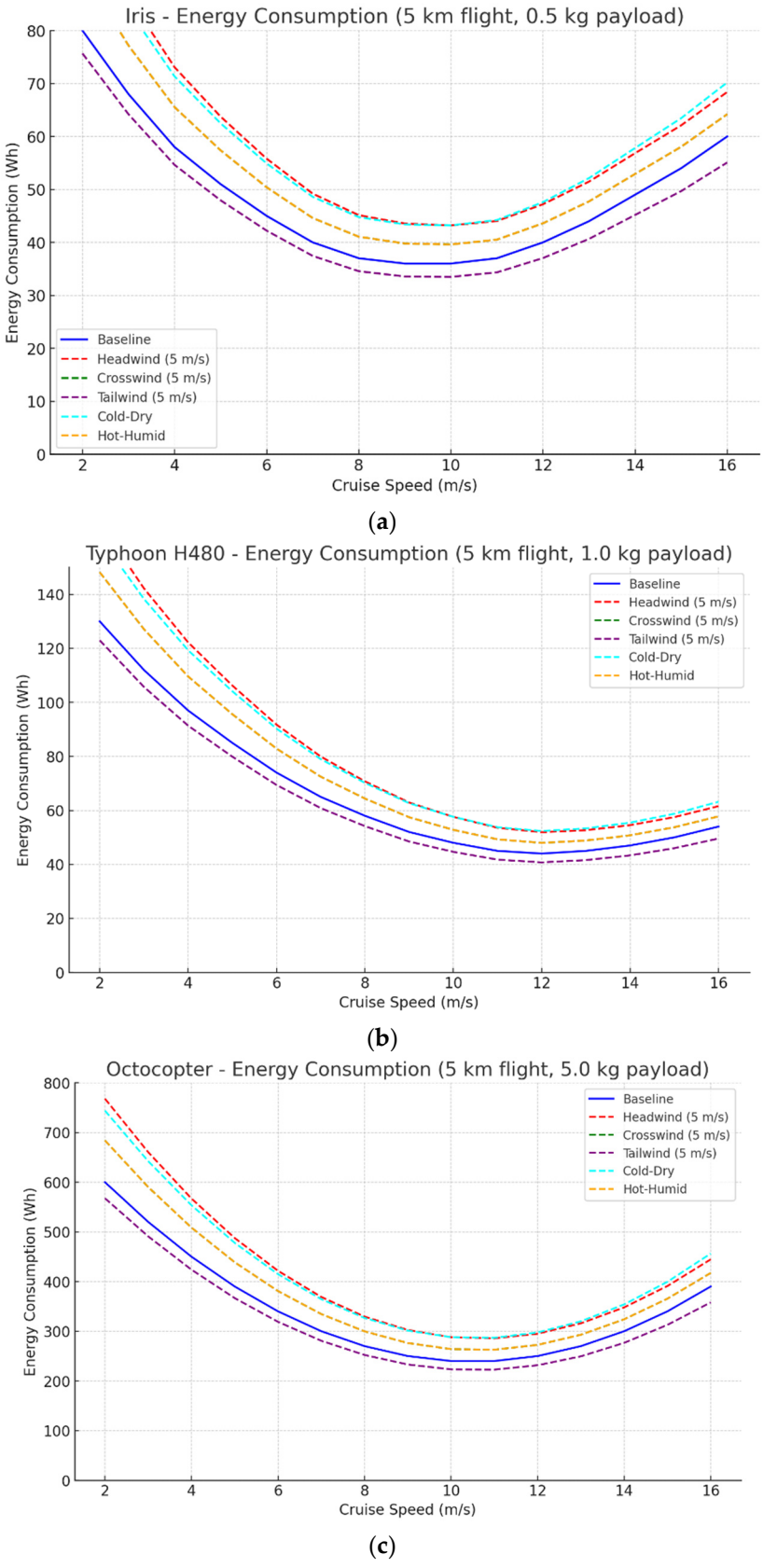

Figure 3. Effect of environmental variables on drone energy consumption under different payloads: (**a**) Iris with 0.5 kg, (**b**) Typhoon H480 with 1.0 kg, and (**c**) Octocopter with 5.0 kg.

For the Iris, the lowest energy consumption occurred between 9 and 10 m/s, with a baseline of approximately 36 Wh. Under a 5-m/s headwind, energy consumption increased by 10–20%, and in cold–dry conditions, it rose to approximately 55 Wh. Conversely, tailwind conditions improved

 doi:10.20944/preprints202604.0751.v1

efficiency, reducing consumption to approximately 34 Wh [33]. The Typhoon H480 showed a minimum baseline energy use of approximately 44 Wh at approximately 10 m/s. Headwind and cold–dry conditions raised this to 55–60 Wh. Crosswind added modest drag, increasing consumption to 52–54 Wh, whereas tailwinds reduced energy use to approximately 40–42 Wh [22,34]. For the Octocopter, baseline consumption was approximately 240 Wh at 10 m/s. Exposure to headwind and cold–dry conditions increased demand to approximately 320 Wh. Tailwind scenarios reduced this to under 230 Wh. The hot–humid scenario, characterized by higher temperatures and lower air density, led to a 10% increase in energy consumption [4].

These findings confirm that environmental factors, particularly wind direction and temperature, substantially affect UAV energy efficiency. The Iris, a lighter drone, exhibited greater sensitivity to these effects, whereas the Octocopter, a heavier drone, though consuming more energy in absolute terms, was less affected. Therefore, accurate energy estimation for UAV delivery must consider payload and environmental conditions [35].

Unlike previous studies in which environmental effects were treated as minor [23,24], the aim of this study was to explicitly quantify energy penalties under adverse scenarios (Table 3). The notably higher relative increase for the Iris under cold–dry conditions (+53%) compared with the Typhoon H480 (+25 to +36%) and Octocopter (+33%) is primarily attributable to the Iris platform's lower absolute baseline energy consumption (approximately 36 Wh). Because the Iris operates at a lower power budget, the combined effect of increased air density (+9.7% at 0 °C), battery-loss factor increase, and headwind-induced drag represents a larger fractional penalty on its baseline. Heavier platforms absorb similar absolute penalties but against much larger baseline values, yielding lower percentage changes. These results extend prior findings by offering simulation-based boundaries such as a 25% consumption increase under headwind, providing design boundaries that can inform operational planning [10,16]. Such levels of detail are rarely integrated into current drone logistics frameworks. The observed penalties highlight the operational importance of environmental condition awareness in UAV mission planning and suggest that energy-adjusted performance metrics warrant consideration in drone logistics frameworks. Additionally, these quantified thresholds under headwind, temperature, and humidity stressors serve as operational boundaries that can guide energy-aware path planning and real-time decision systems. Building on prior studies whose findings identified environmental sensitivity in UAV operations [6,23,24,36], the results of this study provide quantified simulation thresholds under systematically varied scenarios for adverse conditions, enhancing their relevance for operational and regulatory frameworks.

Table 3. Summary of energy consumption (Wh) under environmental scenarios at optimal cruise speed.

Scenario	Iris (Wh)	Change (%)	Typhoon (Wh)	Change (%)	Octocopter (Wh)	Change (%)
Baseline (25 °C, calm)	36	—	44	—	240	—
Headwind (5 m/s)	40–43	+10 to +20	50–52	+14 to +18	270–285	+12 to +19
Tailwind (5 m/s)	~34	−6	40–42	−5 to −7	< 230	−4
Crosswind (5 m/s)	38–40	+6 to +11	52–54	+18 to +23	255–265	+6 to +10
Cold–dry (0 °C + headwind)	~55	+53	55–60	+25 to +36	~320	+33
Hot–humid (40 °C + headwind)	39–41	+8 to +14	47–50	+7 to +14	~264	+10

4. Conclusions

This paper presents a comprehensive, simulation-validated analysis of energy consumption for multirotor UAVs in urban last-mile delivery. Using PX4-Gazebo simulations calibrated with real-world data, three UAV platforms spanning a 10-fold mass range (Iris, Typhoon H480, and Octocopter) were evaluated across varying payloads, cruise speeds, and environmental conditions. Results identified an optimal cruise speed (8–10 m/s) for minimizing energy consumption, with

 doi:10.20944/preprints202604.0751.v1

headwinds increasing demand by up to 25% and combined cold–dry and headwind conditions resulting in increases of up to 53% for lightweight platforms, while a 5-kg payload on the Octocopter reached approximately 350 Wh per 5-km mission.

These findings offer actionable guidance for UAV logistics planning, including fleet operators and delivery companies seeking to minimize per-delivery energy costs, UAV manufacturers optimizing platform design, and policymakers defining energy-aware operational corridors. Specifically, identifying optimal cruise speeds and energy penalties under environmental stressors enables improved flight planning, battery management, and UAV model selection. The operational thresholds established here may serve as an input to broader policy discussions; however, direct application to airspace regulations or carbon accounting frameworks would require additional data on grid carbon intensity and lifecycle emissions beyond the scope of this study. By establishing simulation-validated energy thresholds, the findings of this study contribute an empirical reference point that could inform future energy-aware logistics guidelines and fleet-management strategies.

For payloads between 250 and 500 g, typical of last-mile delivery missions, cruise speeds between 8 and 10 m/s were found to minimize energy consumption without significantly affecting mission duration. Table 4 summarizes the platform-specific optimal cruise speed recommendations derived from this study, providing operators with concrete operational guidance for fleet planning. Therefore, this optimal speed range can serve as a baseline for fleet operational strategies [22]. Furthermore, the validated simulation model supports applications in virtual flight testing, mission planning, routing optimization, and energy estimation. These tools help operators and urban planners reduce field-based trial and error, contributing to more efficient and environmentally responsible drone logistics [37].

Table 4. Platform-specific optimal cruise speed recommendations for energy-efficient last-mile UAV delivery.

Platform	Mass (kg)	Payload range (kg)	Optimal speed (m/s)	Min. energy (Wh)	Recommended application
Iris	1.4	0.1–0.5	9	~30–36	Light parcel delivery (< 500 g), short urban routes
Typhoon H480	1.85	0.5–2.0	10	~44–55	Mid-range commercial delivery, mixed payloads
Octocopter	14	0.5–5.0	8	~180–240	Heavy-lift cargo, medical/rural logistics

All values represent baseline (calm, 25 °C) conditions over a 5-km mission. Under adverse environmental conditions (headwind, cold–dry), operators should apply the energy penalty factors reported in Table 3.

However, this study has several limitations. Simulations assumed single-hop missions and excluded multipackage delivery routes or real-time urban airspace constraints. Direct telemetry validation of the Octocopter model was not possible, as no publicly accessible high-resolution flight dataset currently exists for multirotor platforms in this mass class; field validation of heavy-lift UAV energy models remains an important direction for future work. Environmental conditions were modeled as steady-state, excluding dynamic path adjustments, real-time weather variability, or multi-drop logistics. Although wind, temperature, and humidity were included, higher resolution modeling is needed to assess their cumulative impact under dynamic atmospheric conditions [38]. Future research should explore the scalability of UAV logistics under real-time routing, urban wind modeling, and building-induced turbulence. Lifecycle carbon analysis should include battery recycling, localized manufacturing, and the integration of renewable energy charging infrastructure. Future work should also quantify the Global Warming Potential of the examined UAV platforms across the investigated parameter ranges, enabling direct comparison with conventional delivery vehicle emissions on a per-delivery basis. Comparative studies across diverse global cities accounting for grid carbon intensity and regulatory variance are essential for evaluating the true sustainability

 doi:10.20944/preprints202604.0751.v1

potential of drone delivery systems [39]. Logistics providers such as UPS are already piloting drone delivery as part of broader energy-reduction and sustainability strategies [35].

Future research should build on these findings by incorporating dynamic routing algorithms, real-time environmental data, and heterogeneous UAV fleet coordination. Incorporating region-specific grid carbon intensities and warehouse energy profiles would refine the resolution of lifecycle emissions modeling for drone delivery systems [40]. Addressing scalability challenges will require integrating UAV systems with adaptive routing, shared infrastructure, and region-specific regulatory alignment to enable large-scale feasibility in dense urban networks. Key operational barriers to scalability include fleet charging coordination, airspace congestion, and regulatory access. Despite these barriers, simulation-based mission planning and modular fleet architecture provide practical pathways for scaling UAV delivery in urban environments. Additionally, a social life cycle assessment framework could extend the present findings by quantifying social impacts including human health, energy security, and resource access and translating these into financial metrics to provide a comprehensive techno-economic evaluation of UAV delivery systems across the parameter ranges investigated here.

Author Contributions: Conceptualization, S.C.; methodology, S.C.; software, S.C.; validation, S.C.; formal analysis, S.C.; investigation, S.C.; resources, S.C.; data curation, S.C.; writing—original draft preparation, S.C.; writing—review and editing, S.C.; visualization, S.C. The author has read and agreed to the published version of the manuscript.

Funding: This research received no external funding.

Data Availability Statement: The data supporting the findings of this study are openly available in the dataset by Rodrigues et al. [12] at https://doi.org/10.1038/s41597-021-00930-x. The simulation configuration files and processed data generated during this study are available from the corresponding author upon reasonable request.

Conflicts of Interest: The author declares no conflicts of interest.

Abbreviations

The following abbreviations are used in this manuscript:

BLDC	Brushless Direct Current
ESC	Electronic Speed Controller
GPS	Global Positioning System
LCA	Life Cycle Analysis
MAPE	Mean Absolute Percentage Error
PID	Proportional-Integral-Derivative
RH	Relative Humidity
UAV	Unmanned Aerial Vehicle

References

1. Stolaroff, J.K.; Samaras, C.; O'Neill, E.R.; Lubers, A.; Mitchell, A.S.; Ceperley, D. Energy use and life cycle greenhouse gas emissions of drones for commercial package delivery. *Nat. Commun.* **2018**, *9*, 409. https://doi.org/10.1038/s41467-017-02411-5
2. Kellermann, R.; Biehle, T.; Fischer, L. Drones for parcel and passenger transportation: A literature review. *Transp. Res. Interdiscip. Perspect.* **2020**, *4*, 100088. https://doi.org/10.1016/j.trip.2019.100088
3. Browne, M.; Allen, J.; Leonardi, J. Evaluating the use of an urban consolidation centre and electric vehicles in central London. *IATSS Res.* **2011**, *35*, 1–6. https://doi.org/10.1016/j.iatssr.2011.06.002
4. Figliozzi, M.A. Carbon emissions reductions in last mile and grocery deliveries utilizing air and ground autonomous vehicles. *Transp. Res. Part D Transp. Environ.* **2020**, *85*, 102443. https://doi.org/10.1016/j.trd.2020.102443

 doi:10.20944/preprints202604.0751.v1

5. Goodchild, A.; Toy, J. Delivery by drone: An evaluation of unmanned aerial vehicle technology in reducing CO2 emissions in the delivery service industry. *Transp. Res. Part D Transp. Environ*. **2018**, *61*, 58–67. https://doi.org/10.1016/j.trd.2017.02.017
6. Lee, H.; Shin, Y.; Kim, K. Life cycle environmental impacts of parcel delivery using drones and electric vans. *J. Ind. Ecol*. **2021**, *25*, 269–280. https://doi.org/10.1111/jiec.13105
7. Liu, W.; Liu, Y.; Lu, Y. Optimal route planning for UAVs based on energy consumption. *Sensors* **2017**, *17*, 345. https://doi.org/10.3390/s17020345
8. Abeywickrama, H.V.; Jayawickrama, B.A.; He, Y.; Dutkiewicz, E. Comprehensive energy consumption model for unmanned aerial vehicles, based on empirical studies of battery performance. *IEEE Access* **2018**, *6*, 58383–58394. https://doi.org/10.1109/ACCESS.2018.2873040
9. Dorling, K.; Heinrichs, J.; Messier, G.G.; Magierowski, S. Vehicle routing problems for drone delivery. *IEEE Trans. Syst. Man Cybern. Syst*. **2017**, *47*, 70–85. https://doi.org/10.1109/TSMC.2016.2582745
10. Barry, A.M.; Silva, R.A.; McKinney, K.A. Meteorological impacts on drone operations: Energy and emissions implications. *J. Clean. Prod*. **2021**, *295*, 126427. https://doi.org/10.1016/j.jclepro.2021.126427
11. Meier, L.; Tanskanen, P.; Heng, L.; Lee, G.H.; Fraundorfer, F.; Pollefeys, M. PX4: A node-based multithreaded open source robotics framework for deeply embedded platforms. In Proceedings of the IEEE International Conference on Robotics and Automation (ICRA), Seattle, WA, USA, 26-30 May 2015; IEEE: pp. 6235–6240.
12. Rodrigues, T.A.; Patrikar, J.; Choudhry, A.; Feldgoise, J.; Arcot, V.; Gahlaut, A.; Lau, S.; Moon, B.; Wagner, B.; Matthews, H.S.; Scherer, S.; Samaras, C. In-flight positional and energy use data set of a DJI Matrice 100 quadcopter for small package delivery. *Sci. Data* **2021**, *8*, 155. https://doi.org/10.1038/s41597-021-00930-x
13. Imamov, N.; Abbyasov, B.; Tsoy, T.; Martínez-García, E.A.; Magid, E. Evaluation of a weather plugin in Gazebo: A case-study of a wind influence on PX4-based UAV performance. In International Conference on Interactive Collaborative Robotics; Lecture Notes in Computer Science; Springer: Cham, Switzerland, 2024; Volume 14898. https://doi.org/10.1007/978-3-031-71360-6_26
14. Zhou, D.; Ji, Y.; Wang, J. Energy modeling for multicopter UAVs. *Aerosp. Sci. Technol*. **2020**, *96*, 105543. https://doi.org/10.1016/j.ast.2019.105543
15. Qin, T.; Zhang, G.; Yang, L.; He, Y. Research on the endurance optimisation of multirotor UAVs for high-altitude environments. *Drones* **2023**, *7*, 469. https://doi.org/10.3390/drones7070469
16. Zhang, J.; Campbell, J.F.; Sweeney, D.C., II; Hupman, A.C. Energy consumption models for delivery drones: A comparison and assessment. Transp. Res. Part D Transp. Environ. 2021, 90, 102668. https://doi.org/10.1016/j.trd.2020.102668
17. Kirschstein, T. Comparison of energy demands of drone-based and ground-based parcel delivery services. Transp. Res. Part D Transp. Environ. 2020, 78, 102209. https://doi.org/10.1016/j.trd.2019.102209
18. Harrington, A.M.; Kroninger, C. *Characterization of Small DC Brushed and Brushless Motors*; Technical Report ARL-TR-6389; U.S. Army Research Laboratory: Adelphi, MD, USA, 2013.
19. Zhu, H.; Nie, H.; Zhang, L.; Wei, X.; Zhang, M. Aerodynamic performance of propellers for multirotor unmanned aerial vehicles: Measurement, analysis, and experiment. *Shock Vib*. **2021**, *2021*, 9538647. https://doi.org/10.1155/2021/9538647
20. Abdilla, A.; Richards, A.; Burrow, S. Power and endurance modelling of battery-powered rotorcraft. In Proceedings of the 2015 IEEE/RSJ International Conference on Intelligent Robots and Systems (IROS), Hamburg, Germany, 28 September–2 October 2015; pp. 675–680. https://doi.org/10.1109/IROS.2015.7353445
21. Buck, A.L. New equations for computing vapor pressure and enhancement factor. *J. Appl. Meteorol*. **1981**, *20*, 1527–1532. https://doi.org/10.1175/1520-0450(1981)020<1527:NEFCVP>2.0.CO;2
22. Lu, Z.; Cai, L.; Hu, X.; Zhang, Y.; Deng, R. An energy-efficient logistic drone routing method considering dynamic drone speed and payload. *Sustain.* **2024**, *16*, 4995. https://doi.org/10.3390/su16124995
23. Boucher, J.L.; Chen, R.B. Evaluating the carbon savings potential of drone deliveries. *Transp. Res. Part D Transp. Environ.* **2021**, *95*, 102860. https://doi.org/10.1016/j.trd.2021.102860
24. Cha, S.; Kim, H.; Park, Y. Life cycle CO2 evaluation of urban parcel delivery system with electric vehicles and drones. *Sustain.* **2019**, *11*, 6233. https://doi.org/10.3390/su11226233

 doi:10.20944/preprints202604.0751.v1

25. Gong, H.; Huang, B.; Jia, B.; Dai, H. Modeling power consumptions for multirotor UAVs. *IEEE Trans. Aerosp. Electron. Syst*. **2023**, *59*, 7409–7422. https://doi.org/10.1109/TAES.2023.3287571
26. Bauersfeld, L.; Scaramuzza, D. Range, endurance, and optimal speed estimates for multicopters. *IEEE Robot. Autom. Lett*. **2022**, 7, 2953–2960. https://doi.org/10.1109/LRA.2022.3145063
27. Dahle, L.; Andersson, H.; Christiansen, M.; Speranza, M.G. The pickup and delivery problem with time windows and occasional drivers. *Comput. Oper. Res.* **2019**, *109*, 122-133. https://doi.org/10.1016/j.cor.2019.04.023
28. Chan, Y.; Ng, K.K.; Wang, T.; Hon, K.; Liu, C. Near time-optimal trajectory optimisation for drones in last-mile delivery using spatial reformulation approach. *Transp. Res. Part C Emerg. Technol.* **2025**, *171*, 104986. https://doi.org/10.1016/j.trc.2024.104986
29. Ulmer, M.W. Approximate dynamic programming for same-day delivery with drones. *Eur. J. Oper. Res.* **2020**, *282*, 1058-1070. https://doi.org/10.1016/j.ejor.2019.10.005
30. Moshref-Javadi, M.; Winkenbach, M. UAV last-mile delivery: Review and gaps. *Drones* **2023**, *7*, 77. https://doi.org/10.3390/drones7020077
31. Gutierrez-Franco, E.; Orozco-Rosas, U.; Balderas-Mata, S.E. Drone logistics under energy and time constraints: A simulation study. *Appl. Sci*. **2021**, *11*, 1711. https://doi.org/10.3390/app11041711
32. Li, X.; Tupayachi, J.; Sharmin, A.; Martinez Ferguson, M. Drone-aided delivery methods, challenge, and the future: A methodological review. *Drones* **2023**, *7*, 191. https://doi.org/10.3390/drones7030191
33. Park, S.; Lee, D.; Kim, Y. Analysis of UAV delivery system energy performance in an urban environment. *J. Clean. Prod*. **2018**, *196*, 338–347. https://doi.org/10.1016/j.jclepro.2018.06.041
34. Jung, H.; Clarke, J.-P. Optimal cruise airspeed selection and RTA adjustment in the presence of wind uncertainty. *Transp. Res. Part C Emerg. Technol*. **2024**, *162*, 104613. https://doi.org/10.1016/j.trc.2024.104613
35. Aurambout, J.-P.; Gkoumas, K.; Ciuffo, B. Last mile delivery by drones: An estimation of viable market potential and access to citizens across European cities. *Eur. Transp. Res. Rev*. **2019**, *11*, 1. https://doi.org/10.1186/s12544-019-0368-2
36. Huang, H.; Savkin, A.V.; Huang, C. Drone-assisted last-mile delivery under windy conditions: Zero pollution solutions. *Smart Cities* **2024**, *7*, 134. https://doi.org/10.3390/smartcities7060134
37. Otto, A.; Agatz, N.; Campbell, J.; Golden, B.; Pesch, E. Optimization approaches for civil applications of unmanned aerial vehicles (UAVs) or aerial drones: A survey. *Networks* **2018**, *72*, 411–458. https://doi.org/10.1002/net.21802
38. Rossberg, M.; Dibbern, H.; Werner, C. Model-based investigation of the influence of environmental conditions on the energy supply of multirotor UAVs. *J. Aviat. Technol. Eng*. **2025**, *14*, Article 9. https://doi.org/10.7771/2159-6670.1311
39. Raivi, A.M.; Huda, S.M.A.; Barua, A.; Reza, A.W. Drone routing for drone-based delivery systems: A review of trajectory planning, charging, and security. *Sensors* **2023**, *23*, 1463. https://doi.org/10.3390/s23031463
40. Argonne National Laboratory. *GREET Model*; Energy Systems Division; Argonne National Laboratory: Lemont, IL, USA, 2020.